

# A nalysis of D ilepton Invariant M ass Spectrum in C + C at 2 and 1 A G eV

M . Thom ere<sup>1</sup>, C . Hartnack<sup>1</sup>, G . Wolf<sup>2</sup>, J. A ichelin<sup>1</sup>

<sup>1</sup> SUBATECH

Laboratoire de Physique Subatom ique et des Technologies A ssociees  
Universite de Nantes – IN 2P 3/CNRS – Ecole des Mines de Nantes

4 rue Alfred Kastler,

F-44072 Nantes, Cedex 03, France

<sup>2</sup> KFK I, P.O. Box 49,

H-1525 Budapest Hungary

(D ated: February 9, 2020)

Recently the HADES collaboration has published the invariant mass spectrum of  $e^+e^-$  pairs,  $dN/dM_{e^+e^-}$ , produced in C+C collisions at 2 A GeV. Using electromagnetic probes, one hopes to get in this experiment information on hadron properties at high density and temperature. Simulations show that firm conclusions on possible in-medium modifications of meson properties will only be possible when the elementary meson production cross sections, especially in the pn channel, as well as production cross sections of baryonic resonances are better known. Presently one can conclude that a) simulations overpredict by far the cross section at  $M_{e^+e^-} \approx M_{\rho}^0$  if free production cross sections are used and that b) the upper limit of the  $\rho$  decay into  $e^+e^-$  is smaller than the present upper limit of the Particle Data Group. This is the result of simulations using the Isospin Quantum Molecular Dynamics (IQMD) approach.

## I. INTRODUCTION

Theory predicts since long that the properties of hadrons change if they are surrounded by matter. For baryons this change has been verified in A reactions where the total photon absorption cross section [1] shows a nontrivial dependence on the mass of the target nucleus. This nontrivial dependence has been interpreted as a change of the properties of the nuclear

resonances in matter [2]. It is, however, difficult to assess whether the observed in-medium modifications have to be attributed to a change of the resonance properties or to a change of those of their decay products. Coupled channel calculations provide a means to answer this question but presently neither the data are sufficiently precise nor the theoretical ingredients can be sufficiently well determined in order to allow for firm conclusions even if for some hadrons like the  $\rho$  [3] and  $K^*$  mesons [4] a lot of progress has been made recently.

The strategy is different for both cases. The study of the strange mesons takes advantage of the fact that they have to be produced in a heavy ion reaction, that each strange hadron is accompanied by an anti-strange one and that the production cross sections are phase space dominated. Systematic studies of the excitation function and of the system size dependence of the yields as well as of the modification of the measured  $K^*$  meson spectra as compared to that measured in pp collisions allow for conclusions on the interaction of the  $K^*$ 's with the environment [5].

The  $\rho$  meson can decay into a dilepton pair which – being an electromagnetic probe – does not interact anymore with the nuclear environment. Therefore this dilepton pair carries direct information on the particle at the time point of its decay in the medium. The problem is that many resonances and mesons contribute to the dilepton yield and it is all but easy to determine which particle is at the origin of the dilepton pair. In order to compare data with theory, one has to identify all dilepton sources and their contribution to the dilepton spectra. This superposition of the different sources is called cocktail plot. If it deviates from experiment at least one of the sources is not correctly described and one may start to test how this source is modified by the hadronic environment.

It was the DLS collaboration which first presented dilepton invariant mass spectra in heavy ion collisions at beam energies of around 1 A GeV [6]. The systematic errors of these exploratory experiments have been, however, too large to allow for a detailed conclusion on the behavior of hadrons in matter. Later, at higher (SPS) energies, the CERES/NA 45 collaboration [7] presented spectra, which were not in agreement with the standard cocktail plots. More recently the NA 60 collaboration measured very precisely the invariant mass spectrum of dileptons in the mass region [8]. Two theoretical models have been advanced to explain this difference. Rapp et al. [3] calculated the in-medium modification of the spectral function of the  $\rho$  in hadronic matter. With this in-medium change of the spectral function the theoretical and experimental yields agree. Gallmeister et al. [9] showed that the

discrepancy disappears as well if one adds to the spectrum the emission of the dileptons from a thermal  $q\bar{q}$  annihilation. Thus it is presently debated whether the discrepancy between cocktail plot and data is due to a hadronic or due to a  $q\bar{q}$  annihilation process. To clarify this question it is necessary to study the dilepton production at lower energies where quarks remain bound in hadrons and therefore the process proposed by Galm eister is absent.

Recently the HADES collaboration has published the dilepton invariant mass spectrum for the reaction  $C + C$  at 2 A GeV [10]. At this energy the formation of a quark phase is beyond reach as the analysis of many other observables has shown. It may therefore serve to solve the question of how the meson changes in a hadronic environment provided that it can be proven that all the other ingredients of the cocktail plot are well under control.

It is the purpose of this article to investigate in detail the dilepton invariant mass spectra using one of the presently available programs which simulate heavy ion reactions on an event by event basis, the Isospin Quantum Molecular dynamics (IQMD) approach [11]. The standard version of this program is supplemented for this investigation by all the relevant cross sections and decay rates which may contribute to the invariant mass spectrum of dileptons: np bremsstrahlung, Dalitz and direct decay,  $\rho$  and  $\omega$  decay, Dalitz decay and  $\omega$  Dalitz decay. The main objective is to find out whether the present data are sufficiently precise in order to allow for conclusions on in-medium modifications of the dilepton sources or to identify the obstacles on the way to achieve this goal.

Before we present the results of our simulations we start out with a discussion of our present theoretical and experimental knowledge of all the elementary processes which contribute to the dilepton spectra and of how they are implemented in our simulation program.

## II. ELEMENTARY DILEPTON CROSS SECTIONS

### A. $\omega$ production and decay

#### 1. $\omega$ decay into dileptons

At low invariant mass the overwhelming number of dileptons comes from the decay of  $\omega$  mesons which can disintegrate into dileptons via  $\omega \rightarrow e^+ e^-$ . The mass distribution of a dilepton in a  $\omega$  Dalitz decay is given by [12]:

$$\frac{dN}{dM} = \frac{1}{M} \left(1 + 2\frac{m_e^2}{M^2}\right) \left(1 - \frac{M^2}{m_0^2}\right)^3 \sqrt{1 - 4\frac{m_e^2}{M^2}} \quad (1)$$

$m_0$  is the mass of the  $\phi$ ,  $m_e$  the electron mass and  $M$  that of the dilepton pair. We take the branching ratio  $BR(\phi \rightarrow e^+e^-)$  as 0.01198.

## B. $\phi$ production and decay

In the energy regime which is of interest here, the  $\phi$  production in pp collisions has been well studied by the TAPS [13] and the DISTO collaboration [14]. This can be seen in Fig. 1 which shows on top the distribution of the excess energies in the nucleon nucleon collisions for the reaction  $C+C$  at 2 A GeV. The excess energy  $x$  is defined as

$$x = \frac{P - S}{2M_N - M} \quad (2)$$

We see that excess energies below 0.6 GeV are most relevant for this reaction. In the bottom part of Fig. 1 we display the world data points for  $\phi$  production in elementary NN collisions [13, 14, 15]. Whereas the cross section ( $pp \rightarrow \phi$ ) is known over the whole excess energy interval which is relevant for our investigation the ( $pn \rightarrow \phi$ ) cross section is known only up to an excess energy of  $x = 0.12$  GeV. Thus we have to extrapolate this cross section into the relevant excess energy domain. This extrapolation leaves a lot of freedom even if the  $\phi$  meson production cross section has been measured in heavy ion reactions by the TAPS collaboration. The reason is that in heavy ion reactions a multitude of processes may modify the elementary cross section at the same nominal energy. These processes and the consequences will be discussed later. We parametrize the ( $pn \rightarrow \phi$ ) and ( $pp \rightarrow \phi$ ) cross section by a fit using the form

$$\sigma(x) = ax^b \quad (3)$$

with  $a = 1213.8; a = 162.1; a = 99.6$  and  $b = 1.50, b = -0.08, b = -1.24$  for excess energies of  $x < 283$  MeV,  $283$  MeV  $< x < 651$  MeV,  $x > 651$  MeV for pp collisions and  $a = 25623; a = 324.3; a = 199$  and  $b = 2.03, b = -0.08, b = -1.24$  for excess energies of  $x < 200$  MeV,  $200$  MeV  $< x < 651$  MeV,  $x > 651$  MeV for np collisions assuming that at large excess energies the np cross section is twice the pp cross section. These fits are also displayed in Fig. 1. We parametrize the mass distribution of the  $\phi$  (and thus also mass

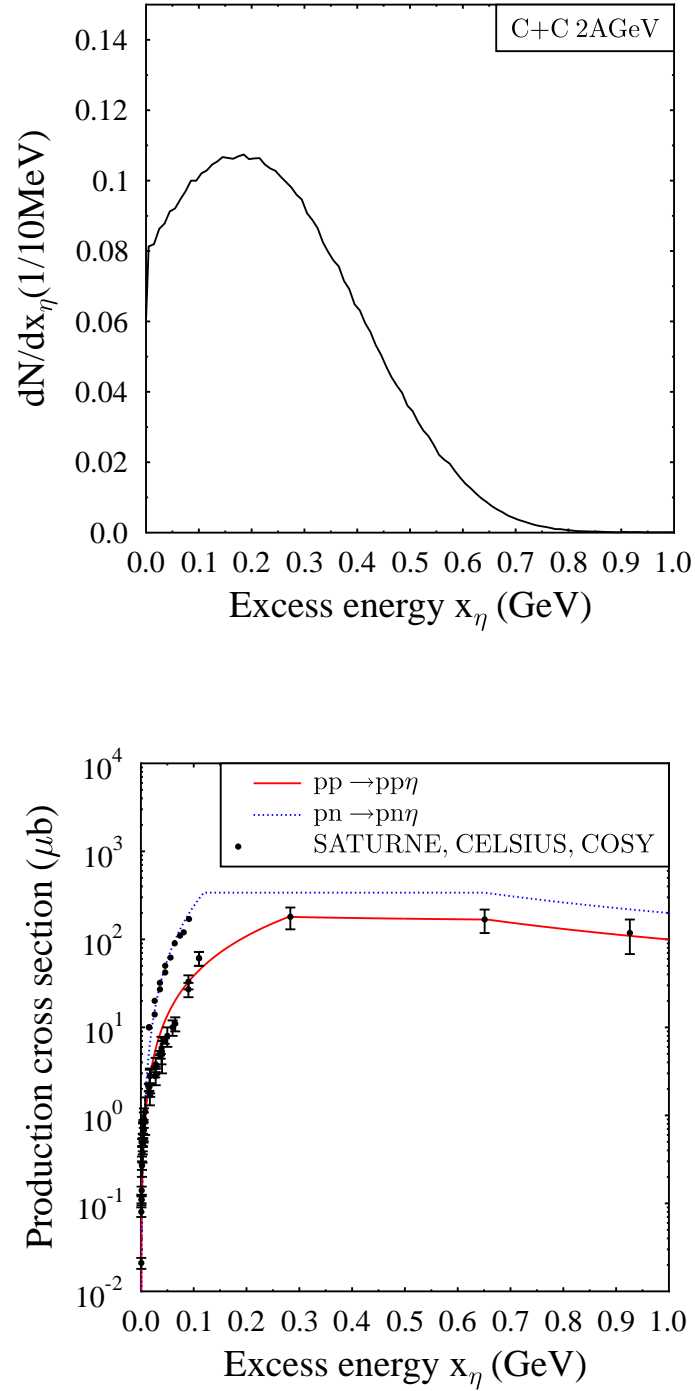


FIG .1: Top: excess energy,  $x_\eta$ , distribution of NN collisions in the reaction  $2 \text{ A GeV C} + \text{C}$ . Bottom : production cross section of the  $\eta$  meson. The solid curves are fits (eq. 3) to the data [13, 16]

distribution of the dileptons from direct decay) by [17]

$$\frac{dN}{dM} = \frac{r \frac{1}{4} \frac{m_e^2}{M^2}}{(m^2 - M^2)^2 + \left[ m \left( \frac{m}{M} \frac{M^2 - 4m_e^2}{(m^2 - 4m_e^2)^{3/2}} \right) \right]^2} \quad (4)$$

with  $m = 0.547 \text{ GeV}$  and  $r = 1.18 \text{ keV}$ .

### 1. Contribution of the $N^*(1535)$

The very detailed experimental investigation of the  $\rho$  production in pp collisions at excess energies of 324, 412, and 554 MeV (corresponding to beam energies of  $E_{\text{beam}} = 2.15, 2.5$  and  $2.85 \text{ GeV}$ ) by the DISTO collaboration [14] allows to identify the different production channels by analyzing the  $p$  invariant mass spectrum. It turned out, as predicted by theory [18, 19], that there are essentially two channels, a direct production channel and a production via the  $N^*(1535)$  resonance. The direct contribution follows the three body phase space for the  $pp \rightarrow pp$  reaction. The experimental mass distribution of the  $N^*(1535)$  resonance created in the reaction  $pp \rightarrow N^*(1535)p$  can be described by a Breit-Wigner distribution of the form [14]:

$$M(\rho) = \frac{A M_R^2}{(M_R^2 - M^2)^2 + M_R^2 x^2(M; M_R)} \quad (5)$$

with

$$x(M; M_R) = b \frac{q(M)}{q(M_R)} + b' \frac{q'(M)}{q'(M_R)} \quad (6)$$

where  $b$  is the branching ratio of the decay  $N^*(1535) \rightarrow N \rho$  (which we assume to be 55%),  $b'$  is the branching ratio of the decay  $N^*(1535) \rightarrow N \pi$  (which counts for 45%).  $q$  and  $q'$  are the momenta of  $\rho$  and  $\pi$  in the frame of the resonance and are given by:

$$q(M; M_N) = \sqrt{\frac{M_N^2 - M^2}{2M_N} \frac{M^2 - M_P^2}{M^2}} \quad (7)$$

and

$$q'(M; M_N) = \sqrt{\frac{M_N^2 - M^2}{2M_N} \frac{M^2 - M_P^2}{M^2}} \quad (8)$$

We note in passing that in reference [14] the square on the  $x$  in eq. 5 has been forgotten. In fig. 2 we display for the three energies which have been measured by the DISTO collaboration [14] the total experimental and theoretical  $p$  invariant mass distribution as well as the different contributions to the theoretical curve. The experimental data are best reproduced

for  $M_R = 1.530 \text{ GeV}$  and  $\Gamma_R = 150 \text{ MeV}$ . As expected, the  $N^*(1535)$  resonance enhances the low invariant mass part as compared to phase space. How the resonance production

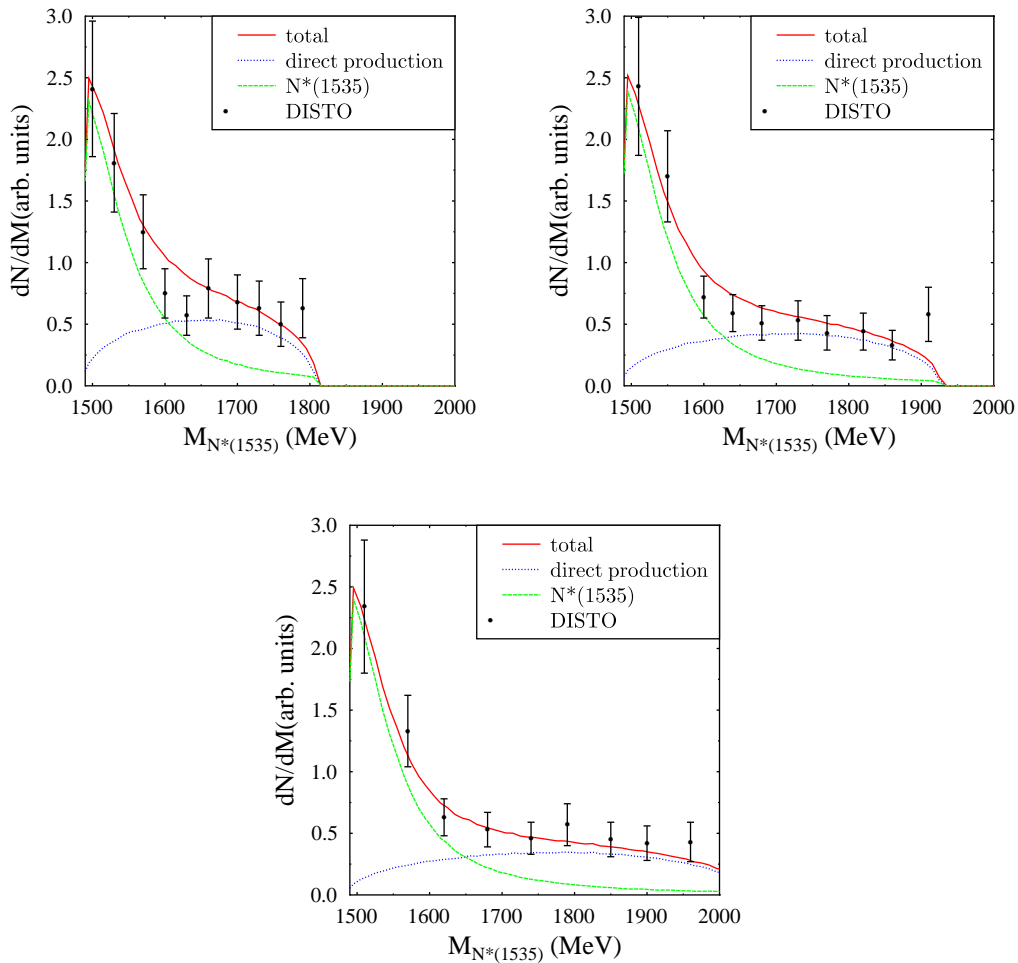


FIG. 2: Simulated invariant mass spectrum of the outgoing proton and the meson in the  $pp \rightarrow p\pi^0$  reaction for three beam energies (2.15 GeV, 2.5 GeV and 2.85 GeV). The curves represent the sum of the contributions from the two production channels of the  $\pi^0$ , the direct production and that via the  $N^*(1535)$  resonance. The data [14] have no absolute normalization. We normalize them here to our result at  $M_{N^*(1535)} = 1500 \text{ MeV}/c^2$

modifies the spectra of proton and meson as compared to the production according to the three body phase space is shown in Fig. 3. On the left hand side we display the center of mass momentum of the  $\pi^0$ , on the right hand side the proton momentum in the  $pp$  rest frame. Choosing these variables allows for a comparison with the experimental results. We see clearly the consequence of the  $N^*(1535)$  resonance production and therefore it will be difficult to

separate the modification of the  $\Lambda$  in the medium from that of the  $N^*(1535)$  resonance. Both will show up as a modification of the dilepton spectra.

## 2. $\Lambda$ decay into dileptons

With a branching ratio of  $6 \cdot 10^3$  [20] the  $\Lambda$  decays into  $e^+e^-$ . The invariant mass distribution of the dilepton pair is given by [12]

$$\frac{dN}{dM} = \frac{1}{M} \left(1 + 2\frac{m_e^2}{M^2}\right) \left(1 - \frac{M^2}{m^2}\right)^3 \sqrt{1 - 4\frac{m_e^2}{M^2}} \quad (9)$$

$m$  is the mass of the  $\Lambda$ ,  $m_e$  the electron mass and  $M$  that of the dilepton pair. It has been shown that this expression has to be multiplied with an electromagnetic form factor. With

$$\left(\frac{dN}{dM}\right)_{\text{tot}} = F(M^2) \frac{dN}{dM} \quad (10)$$

where

$$F(M^2) = \left(\frac{1}{1 - \frac{M^2}{\Lambda^2}}\right)^2 \quad (11)$$

with  $\Lambda = (0.72 \pm 0.09) \text{ GeV}$  one finds good agreement with data [17]. In addition to the three body decay there may also be a two body disintegration into a dilepton pair. The Particle Data Group [20] quotes as an upper limit a branching ratio of  $7.7 \cdot 10^5$ . We include this value in our standard calculation.

## C. $\Lambda$ production and decay

The  $\Lambda$  production in pp collisions for excess energies below 440 MeV has been studied at COSY [21], at SATURNE [22] and by the DISTO [23] collaboration. The cross section as well as our fit of the form  $a x_1^b$  where  $x_1$  is the excess energy in MeV,  $a = (192.204 \pm 8.622)$  and  $b = 1.12182 \pm 0.1077$  is shown in fig. 4. We include in our simulation as well the endothermic ( $\bar{p} + \bar{p} \rightarrow \Lambda + \bar{N}$ ,  $m_{\Lambda} - m_N = 643 \text{ MeV}$ ) reaction  $\bar{p} + \bar{p} \rightarrow \Lambda + \bar{N}$ . Because  $\bar{p}$ 's have usually only a small energy this reaction is less important than the baryonic channel. The experimental data have been parametrized [24] by

$$\sigma_{\bar{p} + \bar{p} \rightarrow \Lambda + \bar{N}} (\text{mb}) = \frac{1.38 \left(\frac{P}{s} - \frac{P}{s_0}\right)^{1.6}}{0.0011 + \left(\frac{P}{s} - \frac{P}{s_0}\right)^{1.7}} \quad (12)$$

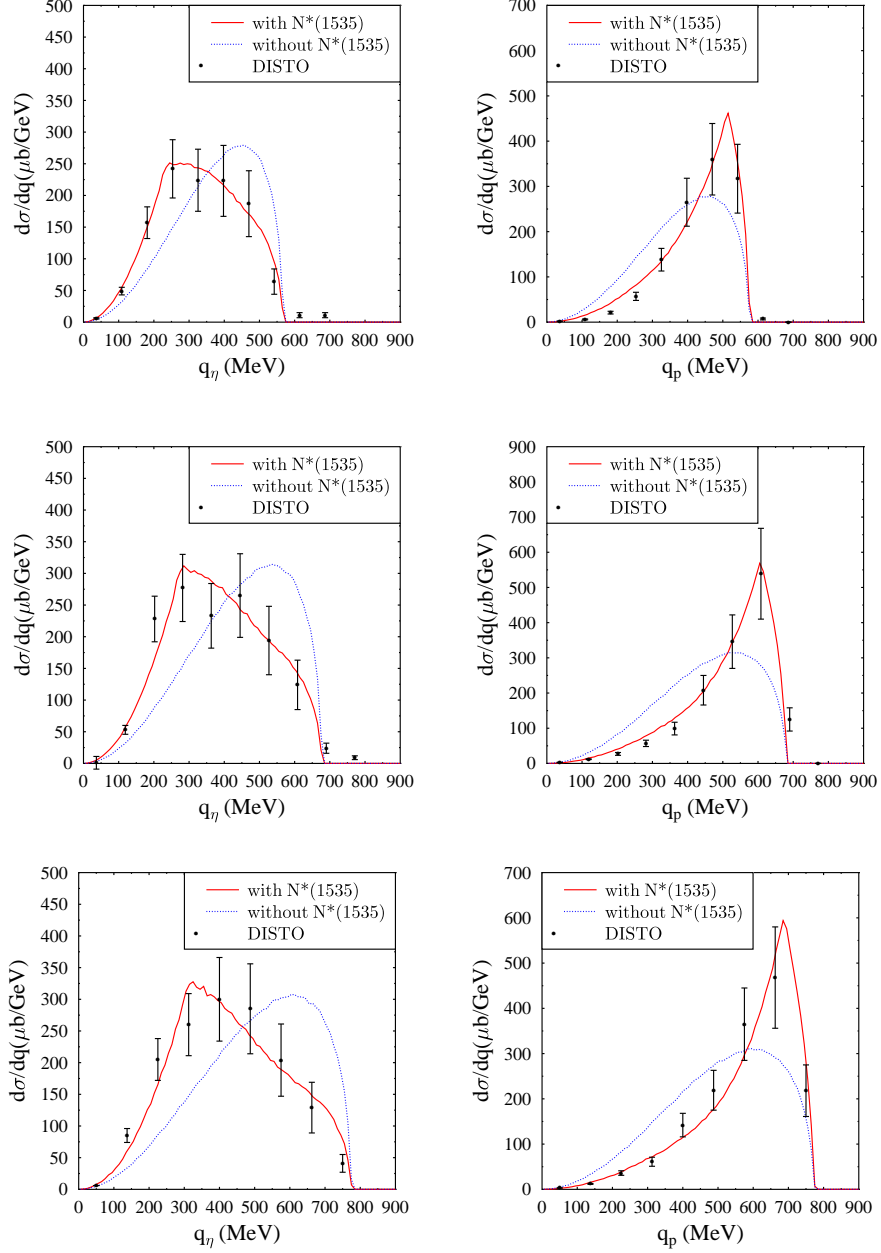


FIG. 3: Differential cross section in IQMD as a function of the center of mass momentum of the meson (left) and as a function of the proton momentum in the pp rest system (right) for  $pp \rightarrow pp$  collisions at different beam energies,  $E_{\text{beam}} = 2.15$  GeV (up),  $E_{\text{beam}} = 2.5$  GeV (middle) and  $E_{\text{beam}} = 2.85$  GeV (down). Solid lines represent production including the contribution of the  $N^*(1535)$  resonance and dashed curves represent the direct production via an uniform three body phase space distribution. The experimental data are from ref. [14]

with  $\sigma$  in mb,  $\sqrt{s}$  and  $\sqrt{s_0}$  in GeV.  $\sqrt{s_0} = m_N + m_\pi$  (1.721 GeV for  $\pi$  in vacuum) is the threshold energy. It has been suggested that the production of the  $\pi^0$  passes by the excitation of baryon resonances [25, 26] where the  $N^*(1535)$  plays a prominent role having a substantial branching ratio into the  $N\pi$  channel [27, 28, 29]. It produces  $\pi$  mesons with masses well below 783 MeV. If this were the case the strong  $\pi N$  coupling would lead to a strong  $s$ -shell contribution to  $d\sigma/dM$  ( $M$  being the invariant mass of the dilepton pair) at invariant masses well below the free  $\pi$  mass peak. This  $s$ -shell  $\pi$  production would even dominate the dilepton spectra up to excess energies of several hundred MeV. Only very recently calculations of the spectral function have been advanced which exploit the available  $N$  and  $N^*$  data in a coupled channel analysis [28, 30].

A  $\pi^0$  experiment was recently performed by the CBELSA/TAPS collaboration. They observed that the pole mass decreases with increasing density of the environment. [31]. For momenta less than 500 MeV/c<sup>2</sup>, they observed an  $\pi^0$  pole mass of  $M = [722^{+2}_{-2}(\text{stat})^{+35}_{-5}(\text{syst})] \text{ MeV}/c^2$  for an average density of  $0.6 \rho_0$ . Unfortunately, no significant measurement of the width was obtained due to the dominance of the experimental resolution. Using this data and the Brown-Rho scaling formula:

$$m_\pi = m_\pi^0 \left(1 - \frac{\rho}{\rho_0}\right) \quad (13)$$

we find  $\rho = 0.13$ . Fig. 5 shows the density distribution at the  $\pi^0$  production points for a C+C collision at 2AGeV. The average density of  $\langle \rho \rangle = 1.394 \rho_0$  is twice as large as for the TAPS experiment. Applying eq. 2 we obtain a wide distribution around the average pole mass of  $M = 641 \text{ MeV}$ .

In our simulation we have the option to use this in-medium mass modification. Because there are no conclusive results on the width we kept the free value of 8 MeV. The mass distribution of the  $\pi^0$  is given by the Breit-Wigner distribution:

$$\frac{dN}{dM} = \frac{r \frac{1}{(1 + 2\frac{m_\pi^2}{M^2})} \frac{1}{4\frac{m_\pi^2}{M^2}}}{\left(m_\pi^2 - M^2\right)^2 + \left[m_\pi \left(\frac{1}{M} \frac{(M^2 - 4m_\pi^2)^{3/2}}{(m_\pi^2 - 4m_\pi^2)^{3/2}}\right)\right]^2} \quad (14)$$

with  $\Gamma = 8 \text{ MeV}$  and  $m_\pi$  as defined in eq. 13.

Another uncertainty is the production of the  $\pi^0$  in pn reactions. In meson exchange models the relative strength of the production in pp and pn reactions depends strongly on the quantum number of the exchanged mesons. Neglecting possible differences due to initial

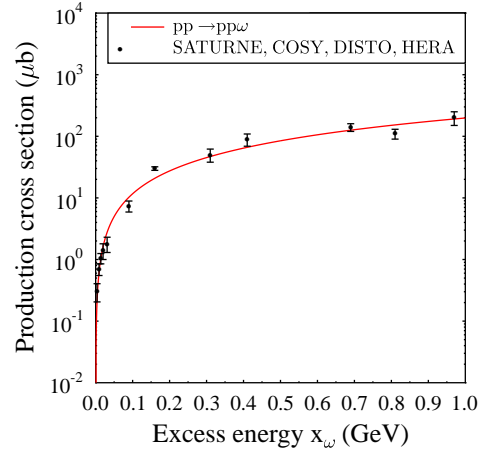


FIG . 4: Production cross section of the  $\omega$  in pp collision up to an excess energy of 440 MeV and our fit of the form  $\sigma = ax_1^b$ . The data are from ref [21, 22, 23].

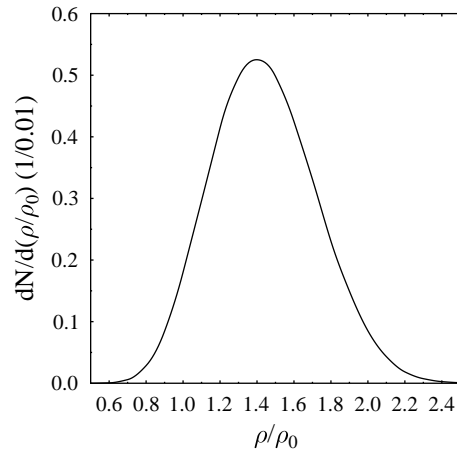


FIG . 5: Distribution of the density at the omega production points in units of the normal nuclear matter density  $\rho_0$  for the reaction  $C + C$  at 2 A GeV.

and  $\pi$  state interactions, we expect  $(\sigma_{pn} - \sigma_{pn'}) / (\sigma_{pp} - \sigma_{pp'}) = 5$ , if only isovector mesons ( $\rho$ ;  $\omega$ ) are exchanged [32]. The two data points for the reaction  $np \rightarrow d\omega$  point toward an enhancement of the  $pn$  cross section as compared to the  $pp$  cross section [32]. The error bars are, however, too large in order to quantify this enhancement. In our simulations we

assume  $(pn \rightarrow pn!) = b (pp \rightarrow pp!)$  with different values of  $b$ .

The  $\omega$  contributes to the dilepton spectrum in two different ways. Either it decays directly into a dilepton pair whose invariant mass equals that of the  $\omega$  meson or the dilepton pair is accompanied by a  $\pi_0$  meson. For the latter channel the dilepton invariant mass distribution has been parametrized by Kroll [12]

$$\frac{dN}{dM} = \frac{1}{M} \left(1 + 2 \frac{m_e^2}{M^2}\right) \left[1 + \frac{M^2}{m_\pi^2 - m_{\pi_0}^2}\right]^2 \left[4 \frac{m_\pi^2 M^2}{(m_\pi^2 - m_{\pi_0}^2)^2}\right]^{3=2} \frac{1}{1 + 4 \frac{m_e^2}{M^2}} \quad (15)$$

with  $M$  being the invariant dilepton mass. This Dalitz type disintegration has to be corrected by an electromagnetic form factor [17]

$$\left(\frac{dN}{dM}\right)_{tot} = F(M^2) \frac{dN}{dM} \quad (16)$$

with

$$F(M^2) = \frac{a^4}{(a^2 - M^2)^2 + a^2 b^2} \quad (17)$$

and  $a = 0.6519 \text{ GeV}$ ,  $b = 0.04198 \text{ GeV}$  in order to be in agreement with data. The branching ratios into the two channels are given by  $5:9 \cdot 10^4$  ( $7:14 \cdot 10^5$ ) for the  $e^+e^-$  ( $e^+e^-$ ) channel [20]. Both, the unknown  $pn$  cross section as well as the little known  $\omega$ -shell contribution at small excess energies make it difficult to predict the  $\omega$  contribution at invariant dilepton masses between 0.6 and 0.8 GeV.

#### D. $\omega$ production and decay

In our simulation the  $\omega$  meson can be produced in three channels:  $NN \rightarrow NN \omega$ ,  $N \rightarrow N \omega$  and  $\pi^+ \rightarrow \pi^0 \omega$ .

The few experimental data points of the total cross section in the  $NN \rightarrow NN \omega$  channel have been fitted by [33]

$$\sigma_{NN \rightarrow NN \omega} (mb) = \frac{0.24 \left(\frac{p}{s} - \frac{p}{s_0}\right)}{1.4 + \left(\frac{p}{s} - \frac{p}{s_0}\right)^2} \quad (18)$$

with  $\frac{p}{s_0} = 2.646 \text{ GeV}$  being the threshold of the reaction. In view of the strong coupling of the  $\omega$  to nuclear resonances this course-grained parametrization has most probably large systematic errors and presents a lower limit to the  $\omega$  production. Other models like URQM D use a parametrization of the resonance production which yield higher yields. For the  $\pi^+N$

! N+ data [28] we use the parametrization of [24]

$$N! N (m b) = \frac{1.5 \left(\frac{P}{s} - \frac{P}{s_0}\right)^{2.2}}{0.0018 + \left(\frac{P}{s} - \frac{P}{s_0}\right)^{3.5}} \quad (19)$$

with  $\frac{P}{s_0} = 1.708 \text{ GeV}$ .

Having a large width and therefore a short lifetime, the meson is an ideal particle to probe whether the nuclear environment changes mesonic properties. If produced in hadronic matter the majority of them decay in matter and therefore the dileptons carry direct information on the in-medium properties. Theory predicts that these properties are different from that of the free meson. Whereas there seems to be now consensus that the width of the meson increases if brought into a nuclear environment [3, 34, 35], the question of how the pole mass changes is still debated. Based on QCD sum rule calculations, Hatsuda and Lee [36] predicted a lowering of the meson mass in a nuclear environment, a suggestion which has later been confirmed by Brown and Rho [37, 38]. More recent and more sophisticated calculations leave, on the contrary, the meson mass almost unchanged [3, 35]. Experimentally the situation is also far from being clear. In pA collisions [39] at 12 GeV a decrease of the meson mass ( $m^*(\rho) = 1.009 m_0$  - about half of the value predicted by theory) and no increase of the width has been reported. The dilepton data in In+In collisions at 158 A GeV [8] are best described using the free meson mass but a considerable broadening of the mass distribution. In contradiction to the theoretical expectations this broadening is almost symmetric around the pole mass. Whether these experimental differences are exclusively due to the different environments (cold nuclear matter in pA reactions, an expanding meson dominated bubble after a possible phase transition from a quark gluon plasma in AA collisions) has not been fully explored yet. It is very difficult to exploit this experimental information for heavy ion reactions at 2 A GeV where theory predicts that most of the mesons are decay products from nuclear resonances, especially of the N(1520) resonance which has a branching ratio of 15-25% into the N channel. For the present status of the theoretical spectral function calculations for the meson we refer to [30, 40].

As for the meson the inconclusive situation of theory and experiment suggest to employ for this exploratory study the free pole mass distribution of the meson:

$$\frac{dN}{dM} = \frac{m^2}{\left(\frac{M^2 - m^2}{m}\right)^2 + \Gamma^2} \quad (20)$$

with  $m = 0.775 \text{ GeV}/c^2$ ,  $m_2 = 0.761 \text{ GeV}/c^2$ ,  $\Gamma = 0.118 \text{ GeV}/c^2$  and the parametrized

free cross sections. For the branching ratio of the  $\Delta$  into dileptons we use  $4.5 \cdot 10^{-5}$ .

### E. $pn$ -bremsstrahlung

In each  $np$  collisions real and virtual photons can be produced. The invariant mass distribution of the  $e^+e^-$  pairs, the decay product of the virtual photon, is given by:

$$\frac{dP(s;M)}{dM} = \frac{1}{3} \frac{1}{M} \frac{s}{e_{cm}^2} \frac{(m_p + m_n)^2}{2} \ln\left(\frac{q_{max} + Q_{max}}{M} \frac{Q_{max}}{q_{max}}\right) \quad (21)$$

with

$$Q_{max} = \frac{s + M^2 - (m_p + m_n)^2}{2\sqrt{s}} \quad (22)$$

$$q_{max} = \frac{Q_{max}}{M^2} \quad (23)$$

$\sqrt{s}$  is the  $np$  center of mass energy,  $e_{cm}$  is the energy of the incoming proton in the  $np$  center of mass system,  $e$  is the electromagnetic coupling constant,  $m_p$  and  $m_n$  the masses of proton and neutron,  $Q_{max}$  the maximal dilepton energy and  $q_{max}$  the maximal dilepton momentum. The bremsstrahlung from  $pp$  collisions is of quadrupole type and can be neglected as compared to the dipole  $pn$  bremsstrahlung.

### F. Dalitz decay

It is not experimentally verified yet whether the Dalitz decay into  $e^+e^-$  of the resonance exists but since it decays into a photon it should also decay into a dilepton. The width of the Dalitz-decay to dileptons of invariant mass  $M$  is determined by QED [41]:

$$\frac{d}{dM^2} = \frac{1}{3} \frac{\Gamma_0(M^2)}{M^2} \quad (24)$$

where

$$\Gamma_0(M^2) = \frac{1}{16} \frac{(M^2; m_N^2; m^2)}{m^2} m_N [\Gamma_{\text{tot}}(M^2) + \Gamma_{\text{ph}}(M^2)] \quad (25)$$

is the total decay rate into a virtual photon with mass  $M$  and

$$(\mathbf{x}; \mathbf{y}; \mathbf{z}) = x^2 + y^2 + z^2 - 2(xy + xz + yz) \quad (26)$$

$\Gamma_{\text{tot}}$  and  $\Gamma_{\text{ph}}$  depend on the form of the interaction. For the decay we take the  $N$  vertex from [42]. Using this interaction we obtain the following matrix elements:

$$M_{\text{ph}} = (efg)^2 \frac{m^2}{9m_N} M^2 4(m_N - m_p)$$

$$M_{\tau} = (efg)^2 \frac{m^2}{9m_N} [\alpha^2 (5m - 3(q_D + m_N)) - M^2 (m + m_N + q_D)] \quad (27)$$

with

$$f = 1.5 \frac{m + m_N}{m_N (m_N + m)^2 - M^2}; \quad (28)$$

$q_D$  the energy of the dilepton pair in the center of mass,  $e$  the electric charge and  $g = 2.72$  is the coupling constant fitted to the photonic decay width  $\Gamma_0(0) = 0.72 \text{ MeV}$  [43].

### III. THE C+C REACTION AT 2 AND 1 AGeV

For the simulation of the heavy ion reaction we use the standard IQMD program to which the above mentioned cross sections have been added. The details of this program can be found in [11]. The presented results are impact parameter averaged and have been corrected for the experimental mass resolution and acceptance with a program provided by the HADES collaboration. We have neglected in our calculation the reabsorption cross section of the mesons which is of the order of 20 mb [44] in our kinematic domain but of little importance for such a light system. Fig. 6 shows the result of the standard simulation set up:  $(np \rightarrow np) = 2 (pp \rightarrow pp)$ ,  $(np \rightarrow pn) = 5 (pp \rightarrow pp)$ ,  $M_{\tau} = M_{\tau}^0$  and the branching ratio  $BR(\tau \rightarrow e^+e^-) = 7.7 \cdot 10^5$ . We see first of all that with the resolution of the HADES experiment the direct decay would yield a visible peak which is not present in the data. Therefore the upper limit has to be lower than that quoted by the Particle Data Group. We see as well that the simulations overpredict the yield in the region of the free  $\tau$  mass. This confirms the result of the simulations with other programs which have been published by the HADES collaboration [10]. On the contrary, the simulations reproduce well the mass region in which the lepton pairs are coming dominantly from the decay and from pnbremsstrahlung. If the experimentally unknown  $(np \rightarrow pn)$  equals  $(pp \rightarrow pp)$  the yield in the  $M_{\tau}$  mass region would be strongly reduced and would be consistent with the experimental data as can be seen in Fig. 7. We obtain the same agreement with data if we take  $(np \rightarrow pn) = 5 (pp \rightarrow pp)$  but assume in addition that the mass of the  $\tau$  decreases in the medium according to eq. 13, as indicated by the CBELSA/TAPS results [31]. This can be seen in Fig. 8. The experimental error bars are presently that large that also simulations with  $(np \rightarrow pn) = (pp \rightarrow pp)$  and an in medium  $\tau$  mass are compatible

with the experimental results, as seen in Fig. 9. Therefore, without further information on  $(np \rightarrow \eta)$  heavy ion reactions will not reveal any information on in-medium modifications of the  $\eta$  meson.

If we assume  $\sigma(np \rightarrow \eta) = 2 \sigma(pp \rightarrow \eta)$  in the region where no data on the  $(np \rightarrow \eta)$  cross section is available (only 5% of the  $\eta$  are produced at an energy where experimental information on this cross section is available), we underpredict slightly the yield in this mass region as seen in Fig. 10. Because the bremsstrahlung spectrum is well under control one can conclude that if the mass of the  $\eta$  does not change in matter  $(np \rightarrow \eta)$  has to be significantly larger than  $(pp \rightarrow \eta)$  at excess energies above 100 MeV. As for the  $\eta$  meson possible in-medium changes of the  $\eta$  meson require a detailed study of its production in the pn channel.

Thus the C+C data at 2 A GeV show interesting new physics which is not compatible with the input of state of the art transport codes. Without further information on the elementary cross sections with a neutron in the entrance channel it will not be possible to identify the origin of this discrepancy because a modification of the mass of the mesons in the medium yields the same effect as a change of the (experimentally unknown) cross section in the np channel.

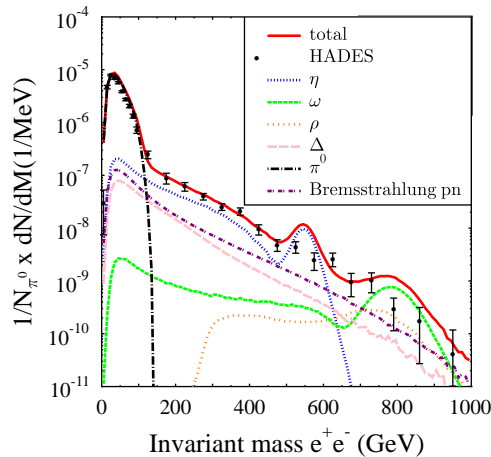


FIG. 6: The invariant mass spectrum of the HADES collaboration as compared with IQMD simulations for C+C at 2 A GeV using  $\sigma(np \rightarrow \eta) = 2 \sigma(pp \rightarrow \eta)$ ,  $\sigma(np \rightarrow \eta) = 5 \sigma(pp \rightarrow \eta)$ ;  $M_{\eta} = M_{\eta}^0$  and the branching ratio  $\mathcal{B}(\eta \rightarrow e^+e^-) = 7.7 \cdot 10^{-5}$  (model A).

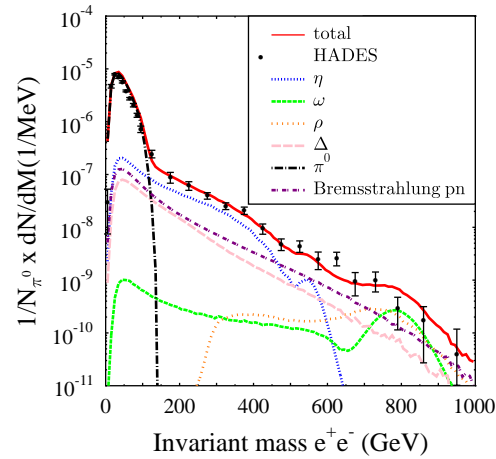


FIG . 7: The invariant mass spectrum of the HADES collaboration as compared with IQMD simulations for C+C at 2AGeV using  $(np \rightarrow np) = 2 (pp \rightarrow pp)$ ,  $(np \rightarrow np!) = (pp \rightarrow pp!)$ ,  $M_{\pi^0} = M_{\eta}^0$  and the branching ratio  $(\pi^0 \rightarrow e^+e^-) = 7.7 \cdot 10^{-6}$  (model B).

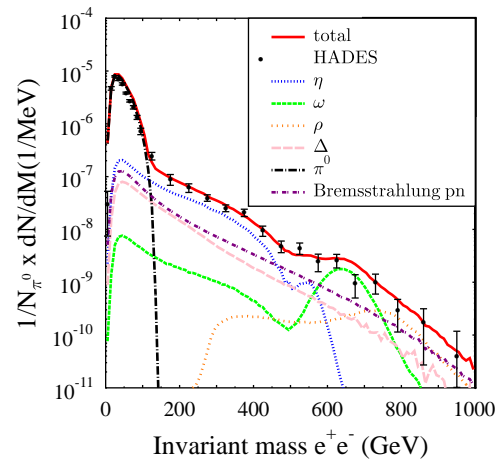


FIG . 8: The invariant mass spectrum of the HADES collaboration as compared with IQMD simulations for C+C at 2AGeV using  $(np \rightarrow np) = 2 (pp \rightarrow pp)$ ,  $(np \rightarrow np!) = 5 (pp \rightarrow pp!)$ ,  $M_{\pi^0} = M_{\eta}^0$  ( $\Gamma_{\pi^0 \rightarrow e^+e^-} = 0$ ) and the branching ratio  $(\pi^0 \rightarrow e^+e^-) = 7.7 \cdot 10^{-6}$  (model C).

Lowering the energy to 1AGeV the importance of the different channels changes and a comparison between the 2 and 1AGeV data will elucidate part of the physics. Because the

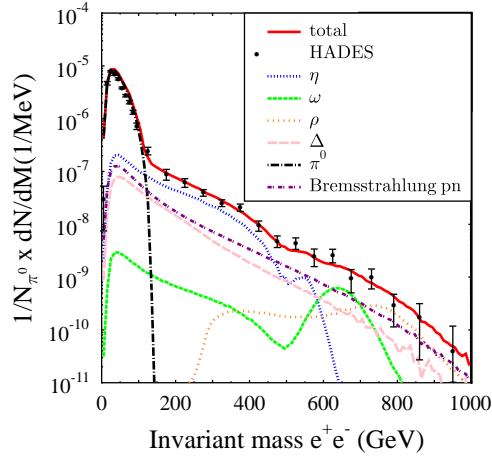


FIG. 9: The invariant mass spectrum of the HADES collaboration as compared with IQMD simulations for C+C at 2A GeV using  $(np \rightarrow np) = 2 (pp \rightarrow pp)$ ,  $(np \rightarrow np!) = (pp \rightarrow pp!)$ ,  $M_{\pi^0} = M_{\pi^0} (1 \pm 0.13 = 0)$  and the branching ratio  $(\pi^0 \rightarrow e^+e^-) = 7.7 \cdot 10^{-6}$  (model E).

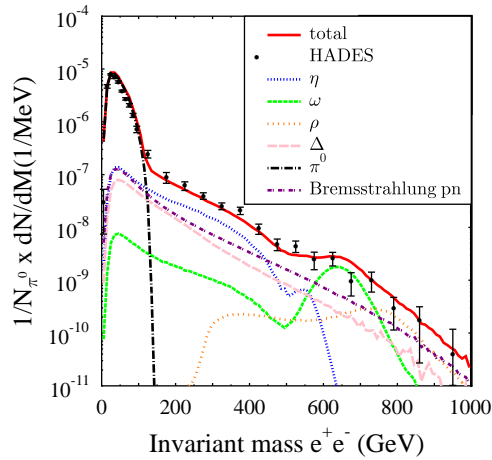


FIG. 10: The invariant mass spectrum of the HADES collaboration as compared with IQMD simulations for C+C at 2A GeV using  $(np \rightarrow np) = (pp \rightarrow pp)$ ,  $(np \rightarrow np!) = 5 (pp \rightarrow pp!)$ ,  $M_{\pi^0} = M_{\pi^0} (1 \pm 0.13 = 0)$  and the branching ratio  $(\pi^0 \rightarrow e^+e^-) = 7.7 \cdot 10^{-6}$  (model D).

experimental data are divided by the number of  $\pi^0$  the spectra for the pions change only little due to the acceptance corrections. The same is true for the Dalitz decay. The yield

of  $e^+e^-$  pairs from Dalitz decay and bremsstrahlung are lower, on the contrary, and the  $\pi^0$  production is practically absent due to the lack of energy (even if one takes into account that the Fermi momentum may create a larger  $\sqrt{s}$  value than in NN collisions at the same beam energy). Fig. 11 displays our filtered and acceptance corrected results. In the intermediate mass region the Dalitz decay and bremsstrahlung have gained importance and are of the same order of magnitude. Dilepton pairs from Dalitz decay are less frequent and are not dominant anymore in the intermediate mass region. At this energy about 35% of the come from a  $\sqrt{s}$  region where the np production cross section is known. So the uncertainty in this channel is reduced but still present. In the standard set up of the simulations the dilepton invariant mass spectrum at intermediate masses has always a strong component of the bremsstrahlung which gives about 50% of the yield. At invariant masses of around 200 MeV the Dalitz decay contributes the other 50% - if it exists. The data at 1 A GeV should therefore allow to deduce an upper limit of the Dalitz decay. At higher invariant masses it is the decay which contributes the other 50%. If we assume that  $(np \rightarrow np) = (pp \rightarrow pp)$  the yield becomes that low that its influence on the spectrum is hardly visible. If we lower

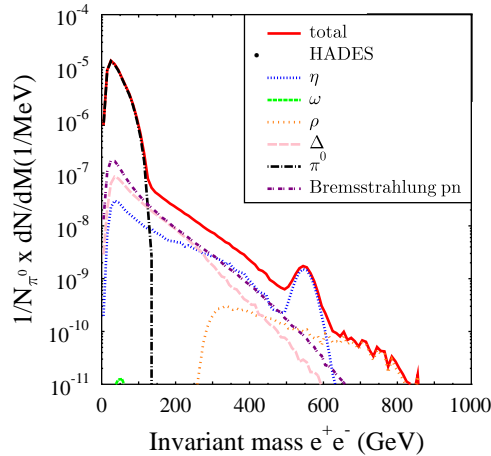


FIG. 11: The invariant mass spectrum of IQMD simulations for C+C at 1 A GeV using  $(np \rightarrow np) = 2 (pp \rightarrow pp)$ ,  $(np \rightarrow np!) = 5 (pp \rightarrow pp!)$ ,  $M_{\pi^0} = M_{\eta}^0$  and the branching ratio  $(\pi^0 \rightarrow e^+e^-) = 7.7 \cdot 10^{-5}$ .

the in medium  $\pi^0$  mass we see a larger  $\pi^0$  production cross section but it remains a small contribution to the total yield, as seen in Fig. 12.

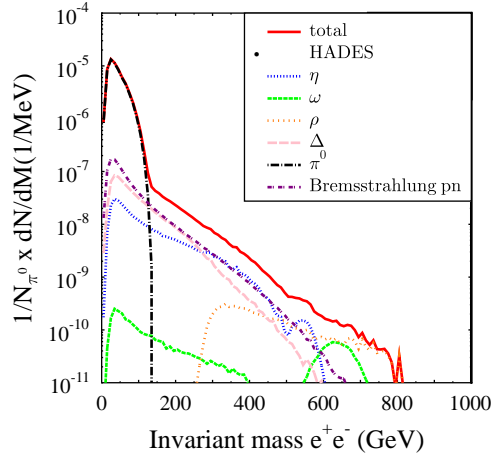


FIG. 12: The invariant mass spectrum of IQMD simulations for C+C at 1AGeV using  $(np \rightarrow np) = 2$  ( $pp \rightarrow pp$ ),  $(np \rightarrow np!) = 5$  ( $pp \rightarrow pp!$ ),  $M_1 = M_1^0 (1 - 0.13 = 0)$  and the branching ratio  $(\Delta \rightarrow e^+e^-) = 7.7 \cdot 10^{-6}$ .

It is interesting to see in detail the differences between elementary collisions at  $\sqrt{s} = 2.697$  GeV and heavy ion collisions at the same nominal energy which show the large  $\sqrt{s}$  distribution of the NN collisions displayed in Fig. 13. There we see two peaks. The high energy peak is due to collisions between projectile and target nucleons, whereas the low energy peak is due to collisions among either projectile or target nucleons. The latter collisions contribute only to the bremsstrahlung and to the  $\pi^0$  part of the dilepton spectrum. Due to rescattering the maximum of the distribution of the primary collisions is shifted toward a lower  $\sqrt{s}$  value. The key quantities of this comparison are summarized in table I. The first line shows the average  $\sqrt{s}$  value of all collisions above threshold. For the  $\Delta$  this value is slightly below, for the  $\pi^0$  - due to the larger threshold - slightly above the value for elementary collisions. Also the average number of collisions in C+C reactions depends on the particle type as seen in the second line. For the  $\Delta$  production we find 4.65 collisions above threshold for the  $\Delta$  production 2.32. For the standard scenario ( $m_1 = m_1^0$ ,  $BR(\Delta \rightarrow e^+e^-) = 7.7 \cdot 10^{-6}$ ;  $(np \rightarrow np) = 2$  ( $pp \rightarrow pp$ ) and  $(np \rightarrow np!) = 5$  ( $pp \rightarrow pp!$ )), we display in the third and the fourth line the average production cross section in np and pp collisions in the heavy ion reaction as compared to the elementary reaction. For the  $\Delta$  the average  $(pp \rightarrow pp)$  and  $(np \rightarrow np)$  are lower in CC collisions than in elementary ones.

This decrease has two origins: firstly the lower  $\langle p_{\text{coll}}^- \rangle_{\text{threshold}}$  and secondly the form of the production cross section which has a maximum at around  $p_{\text{s}}^- = 2.697 \text{ GeV}$  and stays almost constant at higher energies. For the  $\rho$  meson the situation is completely different. The elementary cross section increases with energy for all relevant energies and the average  $p_{\text{s}}^-$  value in C+C is larger than that in elementary collisions. Therefore np as well as pp collisions in the heavy ion reaction produce more  $\rho$  mesons than elementary collisions at the same nominal energy. Consequently the enhancement factor of  $\rho$  and  $\rho$  mesons in heavy ion collisions is very different.

For the 1 A GeV reaction (table II) the situation is very different. The  $p_{\text{s}}^-$  distribution of the collision in C+C is displayed in fig. 14. In elementary NN collisions at the same energy neither  $\rho$  nor  $\rho$  mesons can be produced ( $p_{\text{s,threshold}}^- \rho = 2.659 \text{ GeV}$  and  $p_{\text{s,threshold}}^- \rho = 2.424 \text{ GeV}$ ). However, with the Fermi momentum, in C+C collisions subthreshold  $\rho$  and  $\rho$  production is possible. Due to the larger threshold  $\rho$  production is suppressed with respect to the  $\rho$  production. The production cross section at this energy tests the Fermi motion in the simulations which is not easy to model in semi-classical simulation codes. Therefore systematic errors reduce the predictive power for the meson production at this energy, but in between a factor of two the results are certainly trustworthy.

In summary we have shown that the dilepton spectrum measured by the HADES collaboration in the reaction 2 A GeV C+C at invariant masses above 600 MeV is not compatible with the standard scenario of simulation programs which uses free cross sections and free meson masses. Introducing a medium modification of the  $\rho$  mass or lowering the unknown  $pn \rightarrow \rho$  cross section brings the calculation in agreement with data. The extrapolation from elementary cross section at the same nominal energy to heavy ion reactions is all but trivial. It depends on the threshold and on the energy dependence of the cross section. Before the elementary production cross sections in pn reactions are not determined and before the cross sections for baryonic resonances are not better known heavy ion data do not provide the desired information on possible in medium modification of the meson properties.

Acknowledgment: We acknowledge valuable discussions with M. Bleicher, R. Holzmann, W. Kuhn and J. Stroth and thank the HADES collaboration for providing us with the `lter` routines. G. Wolf acknowledge partial support by the grants T 48833 and T 47347.

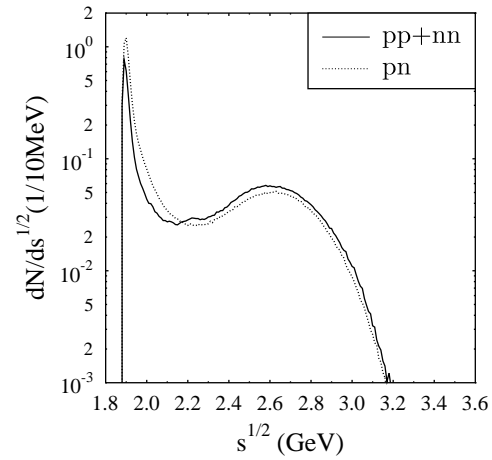


FIG .13: Distribution of  $\bar{p}$  of NN collisions in a C + C reaction at 2 AG eV

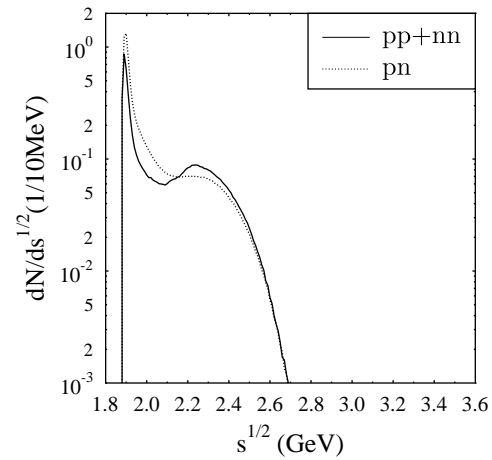


FIG .14: Distribution of  $\bar{p}$  of NN collisions in a C + C reaction at 1 AG eV

---

[1] N. Bianchi et al, Phys. Rev. C 54 (1996) 1688

V. Muccifora et al. Phys. Rev. C 60 (1999) 064616

B. K rusche, S. Schadm and, Prog Part Nucl Phys. 51 (2003) 399-485

[2] M. M. Giannini and E. Santopinto Phys. Rev. C 49 (1994) R1258

Particle				!		
Collision	p+p	p+n	C+C	p+p	p+n	C+C
$\langle \bar{p}_{S_{coll}} \rangle_{threshold}$	2.697	2.697	2.677	2.697	2.697	2.811
$N_{coll} \rangle_{threshold}$	1	1	4.65	1	1	2.32
$h_{prod}^{C+C} (b)$	115	304	203	23.8	115	66.5
$h_{prod} (b)$	175	359		4.90	24.51	
Multiplicity	$3.89 \cdot 10^3$	$8.37 \cdot 10^3$	$2.25 \cdot 10^2$	$2.36 \cdot 10^4$	$5.57 \cdot 10^4$	$3.6 \cdot 10^3$

TABLE I: Comparison of the average number of collisions above threshold, of the average production cross section per NN collision in CC collisions, the cross section in elementary pp and pn reactions and the multiplicity in pp, pn and CC collisions at a beam energy of 2 A GeV for and ! mesons.

Particle				!		
Collision	p+p	p+n	C+C	p+p	p+n	C+C
$\langle \bar{p}_{S_{coll}} \rangle_{threshold}$	x	x	2.498	x	x	2.711
$N_{coll} \rangle_{threshold}$	x	x	0.812	x	x	0.0176
$h_{prod}^{C+C} (b)$	30.2	146.3	84.7	7.11	38.3	22.66
$h_{prod} (b)$	0	0		0	0	
Multiplicity	0	0	$1.61 \cdot 10^3$	0	0	$8.34 \cdot 10^6$

TABLE II: Comparison of the average number of collisions above threshold, of the average production cross section per NN collision in CC collisions, the cross section in elementary pp and pn reactions and the multiplicity in pp, pn and CC collisions at a beam energy of 1 A GeV for and ! mesons.

- M. Hirata, N. Katagiri, K. Ochi, T. Takaki, Phys. Rev. C 66 (2002) 014612
- [3] R. Rapp and J. Wambach, Adv. Nucl. Phys. 25 (2000) 1 (hep-ph/9909229)
- [4] C. L. Korpa, M. F. M. Lutz, Acta Phys. Hung. A 22 (2005) 21 and references therein
- [5] C. Hartnack, J. Aichelin, J. Phys. G 30 (2004) S531
- C. Hartnack, Habilitation, nucl-th/0507002
- [6] R. J. Porter et al. Phys. Rev. Lett. 79 (1997) 1229

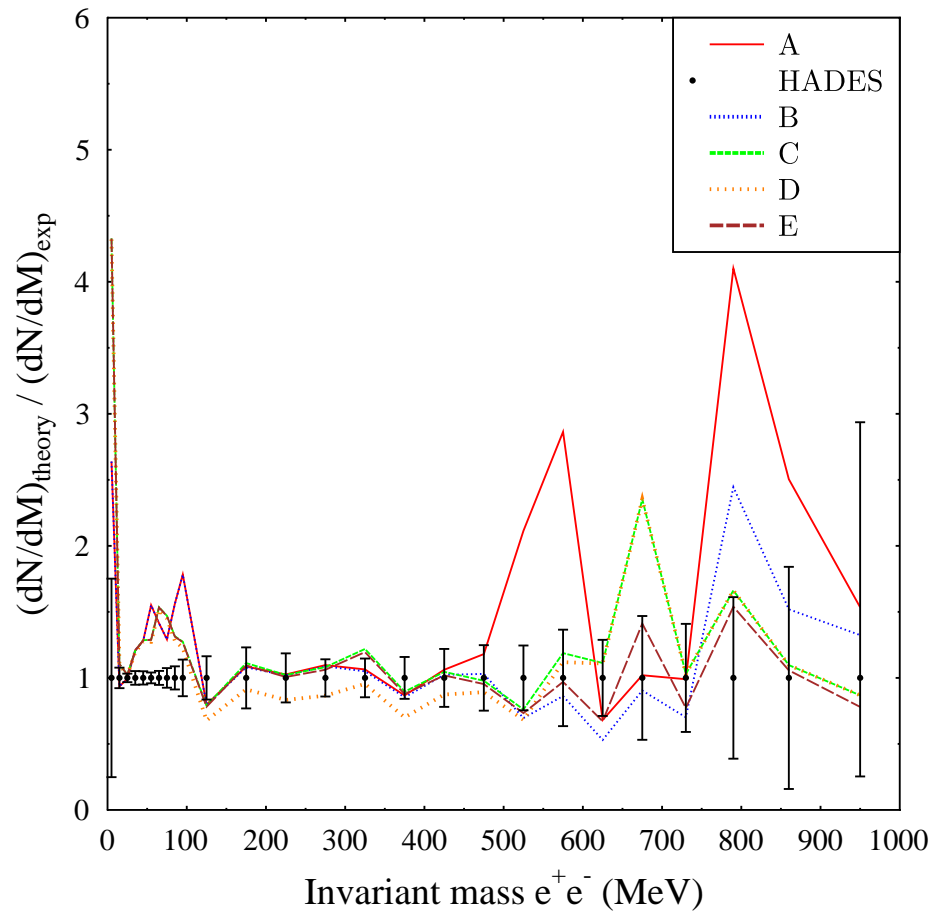


FIG . 15: Distribution of the ratio theory/exp for the C + C reaction at 2 A GeV

G . Roche Phys. Lett. B 226 (1989) 228

[7] D . Miskowiec, Plenary talk in Quark Matter 2005, Budapest, nucl-ex/0511010

[8] R . A Mankiet al. Phys.Rev.Lett. 96 (2006) 162302

[9] K . Gallmeister, B . Kampfer, O . Pavlenko and C . Gale Nucl. Phys. A 688 (2001) 939

[10] I.Frohlich et al., nucl-ex/0610048

[11] C . Hartnack et al. Eur. Phys. J. A 1 (1998) 151.

[12] N M . Kroll and W . Wada, Phys. Rev., Volume 98, p. 1355 (1955)

[13] P Miska et al, Phys. Rev. C 69, (2004) 025203

Model	$BR(\mu^+e^+e^-)$	medium	$\frac{pn!pn!}{pp!pp!}$	$\frac{pn!pn}{pp!pp}$
A	$7.7 \cdot 10^{-5}$	vacuum	5	2
B	$7.7 \cdot 10^{-6}$	vacuum	1	2
C	$7.7 \cdot 10^{-6}$	in-medium modification	5	2
D	$7.7 \cdot 10^{-6}$	in-medium modification	5	1
E	$7.7 \cdot 10^{-6}$	in-medium modification	1	2

TABLE III: Definition of the various parameters for the IQMD simulations

- [14] F. Balestra et al., Phys. Rev. C 69 (2004) 064003
- [15] V. Flaminio, W. G. Moorhead, D. R. O. Morrison, N. Rivoire, Compilation of cross sections III : p and p (1984)
- [16] K. Nakayama, J. Speth and T.-S. H. Lee, Phys. Rev. C, Volume 65, p. 045210 (2002)
- [17] Hermine K. W. Ohri, Thesis, Low mass dimuon production in proton-nucleon collisions at 400 GeV at the CERN-SPS (2004)
- [18] M. T. Pena, H. Garcilazo, and D. O. Riska, Nucl. Phys. A, Volume 683, p. 322 (2001)
- [19] K. Nakayama, J. Speth, and T.-S. H. Lee, Phys. Rev. C, Volume 65, p. 045210 (2002)
- [20] S. Eidelmann et al., Review of Particle Physics Phys. Lett. B 592 (2004) 1
- [21] S. Abd El-Samad et al., Phys. Lett. B 522 (2001) 16
- [22] F. Hibou et al. Phys. Rev. Lett. 83 (1999) 492
- [23] F. Balestra et al., Phys. Rev. C 63 (2001) 024004
- [24] G. Wolf, private communication
- [25] K. T. Sushina, and K. Nakayama, Phys. Rev. C, Volume 68, p. 034612 (2003)
- [26] C. Fuchs et al., Phys. Rev. C 67 (2003) 025202
- [27] M. I. Kivonuchenko et al., Annals Phys. (N.Y.) 296 (2002) 299
- [28] M. F. M. Lutz, G. Wolf, B. Friman, Nucl. Phys. A 706 (2002) 431-496; Erratum *ibid.* A 765 (2006) 431-496
- [29] M. Post et al., Nucl. Phys. A 689 (2001) 753
- [30] K. Gallmeister et al., nucl-th/0608025
- [31] D. Tmka et al., Phys. Rev. Lett. 94 (2005) 192303, nucl-ex 0504010
- [32] S. Barsov et al., Eur. Phys. J. A 21 (2004) 521

- [33] G y. W olf, *Acta. Phys. Polon. B*, Volum e 26, p. 583 (1995)
- [34] R . D . P isarski, *Phys. Rev. D* 52, R 3773 (1995).
- [35] G . Chanfray, R . Rapp and J. W ambach, *Phys. Rev. Lett.* 76, 368 (1996); R . Rapp, G . Chanfray and J. W ambach, *Nucl. Phys. A* 617, 472 (1997).
- [36] T . Hatsuda and S. H . Lee, *Phys. Rev. C* 46, R 34 (1992).
- [37] G . E . Brown, M . Rho, *Phys. Rev. Lett.* 66, 2720 (1991); G . Q . Li, C . M . Ko and G . E . Brown, *Phys. Rev. Lett.* 75, 4007 (1995).
- [38] G . E . Brown and M . Rho, *Phys. Rept.* 363, 85 (2002).
- [39] M . Nankiet al., *Phys Rev Lett.* 96 (2006) 092301, K . O zawa et al., *Phys Rev Lett.* 86 (2001) 5019-5022
- [40] R . Rapp et al., *nucl-th/0608022*
- [41] B E . Lautrup and J. Sm ith, *Phys. Rev. D* 3 (1971) 1122
- [42] G y. W olf, G . Batko, W . Cassing, U . Mosel, K . Niita and M . Schafer, *Nucl. Phys. A* 517 (1990) 615
- [43] G y. W olf et al., *Nucl. Phys. A* 517 (1990) 615
- [44] R . S. Bhalerao and L . C . Liu, *Phys. Rev. Lett.* 54 (1985) 865